

Rpgr^{ORF15} Connects to the Usher Protein Network through Direct Interactions with Multiple Whirlin Isoforms

Rachel N. Wright,¹ Dong-Hyun Hong,^{1,2} and Brian Perkins³

PURPOSE. Mutations in the retinitis pigmentosa GTPase regulator (*RPGR*) gene are a frequent cause of X-linked retinitis pigmentosa. The *RPGR* transcript undergoes complex alternative splicing to express both constitutive (Rpgr^{ex1-19}) and Rpgr^{ORF15} variants. Because functional studies of Rpgr suggest a role in intracellular protein trafficking through the connecting cilia, the goal of this study was to identify potential binding partners for Rpgr^{ORF15} and to identify the domains on whirlin necessary for Rpgr binding.

METHODS. The C-terminus of mouse Rpgr^{ORF15} was used as bait in a yeast two-hybrid system. Whirlin expression was analyzed using RT-PCR and Western blot analysis. Protein-protein interactions were confirmed using in vitro binding assays and coimmunoprecipitation. Subcellular colocalization was analyzed using immunohistochemistry on retinal cryosections.

RESULTS. Yeast two-hybrid analysis identified whirlin, a PDZ-scaffold protein, as a putative binding partner for Rpgr^{ORF15}. The RPGR^{ORF15}-whirlin interaction was confirmed using in vitro binding assays and coimmunoprecipitation from retinal tissue, and both proteins were shown to colocalize in the photoreceptor connecting cilia in vivo. Results from RT-PCR, Western blot analysis, and immunocytochemistry demonstrated that whirlin expressed multiple isoforms in photoreceptors with variable subcellular localization.

CONCLUSIONS. Whirlin expression has been reported in photoreceptors and cochlear hair cells, and mutations in whirlin cause Usher syndrome (USH2D) and nonsyndromic congenital deafness (DFNB31). Because mutations in the 5' end of whirlin are associated with the syndromic phenotype associated with USH2D, the identification of novel N-terminal isoforms in the retina and a novel RPGR^{ORF15}-whirlin interaction provide a potential mechanism for the retinal phenotype observed in USH2D. (*Invest Ophthalmol Vis Sci.* 2012;53:1519-1529) DOI: 10.1167/iovs.11-8845

X-linked retinitis pigmentosa (XLRP) represents the most severe class of retinitis pigmentosa (RP), a group of inherited diseases causing progressive retinal degeneration.^{1,2} RP is characterized by night blindness, progressive loss of visual fields, and eventual blindness, all which result

from photoreceptor cell death and the accumulation of intraretinal pigment-like deposits.³ Mutations in the retinitis pigmentosa GTPase regulator (*RPGR*) gene account for >70% of XLRP and approximately 10% of all RP cases.^{1,2,4} Photoreceptor degeneration occurs after ablation of the *Rpgr* gene in mice⁵ and in dogs with naturally occurring *Rpgr* mutations,⁶ suggesting that photoreceptor survival requires Rpgr. In addition, evidence of early cone photoreceptor defects indicates that Rpgr is necessary for the survival of both types of photoreceptors.^{5,7,8}

Rpgr transcripts undergo complex alternative splicing to generate *Rpgr*^{ex1-19} and *Rpgr*^{ORF15} transcripts^{2,9-11} (Figs. 1A, 1B). *Rpgr*^{ex1-19} variants are widely expressed and contain 19 exons (RPGR^{ex1-19}), whereas the *Rpgr*^{ORF15} variants are preferentially expressed in the retina and contain exons 1-13 plus a large, alternatively spliced C-terminal exon 14/15.^{2,5} Both variants share a common N-terminal domain; however, their remaining C-terminal domains vary considerably.^{1,2,5} The presence of disease-causing mutations within the ORF15 exon suggests that *Rpgr*^{ORF15} variants are functionally significant.²

Rpgr localizes to the photoreceptor-connecting cilium.^{5,9,12} One of the primary defects in mice lacking Rpgr is cone opsin mislocalization in photoreceptors.⁵ Although this suggests that Rpgr regulates protein trafficking through the connecting cilia, the function of Rpgr is poorly understood, and little is known about physiological binding partners.

To further investigate the in vivo function of Rpgr, we used a yeast two-hybrid screen to identify potential interacting partners of Rpgr^{ORF15}. We identified a novel N-terminal variant of whirlin, a putative PDZ scaffold protein expressed in cochlear hair cells and retinal photoreceptors. Whirlin is a member of the Usher protein network, a dynamic complex that includes motor proteins, scaffold proteins, cell adhesion molecules, and transmembrane receptors critical for the development and maintenance of these sensorineural cells.¹³⁻¹⁹ Mutations in the *DFNB31/WHRN* gene encoding whirlin cause the nonsyndromic deafness DFNB31 and Usher syndrome, type 2D (USH2D), an autosomal recessive condition characterized by congenital deafness and RP.^{20,21} The direct association between whirlin and Rpgr^{ORF15} provides a novel mechanism for RP in USH2D.

METHODS

Animals

C57BL/6 mice were obtained from Harlan Laboratories (Houston, TX), and RPGRIP knockout mice were generated by targeted disruption of the *RPGRIP* gene, as previously described.²² All animals were maintained on a 12-hour light/12-hour dark cycle, with food and water ad libitum, and were handled in accordance with the

From the Departments of ¹Veterinary Pathobiology and ³Biology, Texas A&M University, College Station, Texas.

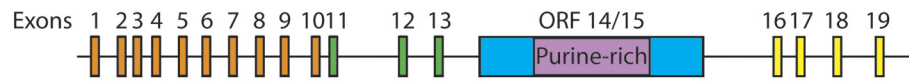
²Deceased, December 24, 2009.

Supported by National Institutes of Health Grant EY14188 (D-HH). Submitted for publication October 21, 2011; revised January 13, 2012; accepted January 28, 2012.

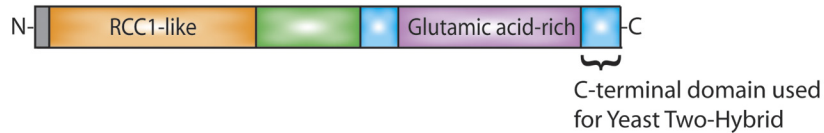
Disclosure: R.N. Wright, None; D.-H. Hong, None; B. Perkins, None

Corresponding author: Brian Perkins, Texas A&M University, 3258 TAMU, College Station, TX 77843; bperkins@mail.bio.tamu.edu.

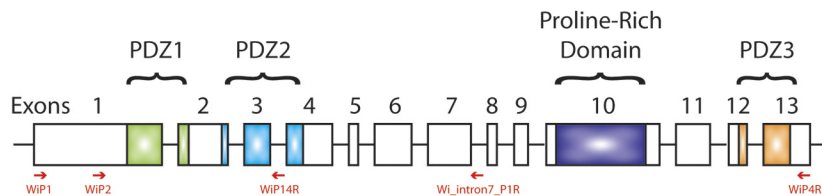
A. RPGR Gene Structure



B. RPGR ORF15 Protein Isoform



C. Whirlin Gene Structure



D. Amplification of whirlin transcripts from retinal cDNA

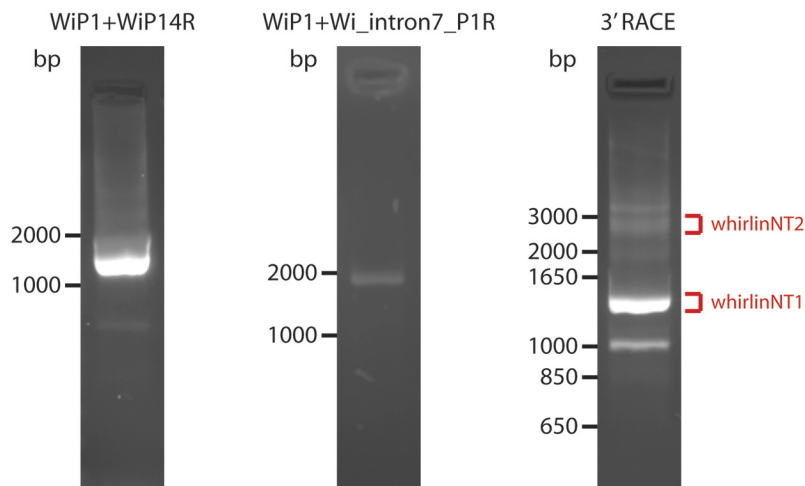


FIGURE 1. Illustration of the *Rpgr* and *whirlin/DFNB31* gene structures, and analysis of *whirlin* expression in the mouse retina at the RNA level. (A) Schematic representation of the *Rpgr* gene structure. Alternative splicing leads to two groups of *Rpgr* transcripts; *Rpgr*^{ex1-19} includes exons 1–13 and exons 16–19, whereas *Rpgr*^{ORF15} includes exons 1–13 plus a large, alternatively spliced ORF 14–15. *Orange*: exons encoding an RCC1-like domain common to all *Rpgr* isoforms. *Green*: remainder of exons common to all *Rpgr* isoforms. *Blue/purple*: exon (ORF 14/15) unique to *Rpgr*^{ORF15}. *Purple*: alternatively spliced region of ORF14/15 encoding glutamic acid-rich domain. (B) Illustration of the *Rpgr*^{ORF15} isoform. All colors correspond to their respective exons shown in A. *Brackets* indicate the location of domain used as bait in the yeast two-hybrid screen. (C) Schematic representation of the *whirlin/DFNB31* gene structure. Whirlin is composed of 13 exons encoding three PDZ domains and a proline-rich region. Exons and encoded domains are drawn approximately to scale. PCR primers used for amplification of *whirlin* transcripts are shown as *red arrows*. (D) Amplification of *whirlin* N-terminal transcripts from C57BL/6 retinal cDNA. *Left/center*: *whirlin* mRNA transcripts were reverse transcribed and amplified using primers shown in Figure 2A. The *whirlinNT1* transcript, which includes intron 3, was amplified by WiP1 and WiP14R, and the *whirlinNT2* transcript, which includes intron 7, was amplified by WiP1 and Wi_intron7_P1R. *Right*: *whirlin* N-terminal transcripts were also amplified by nested PCR of 3' RACE retinal cDNA. Transcripts were first amplified using WiP1 and GeneRacer 3' Primer followed by WiP2 and GeneRacer 3' Nested Primer. The regions excised and used to clone and sequence the *whirlinNT1* and *whirlinNT2* transcripts are indicated by the *red brackets*.

institutional guidelines as approved by the Texas A&M University Institutional Animal Care and Use Committee. Whirlin knock-out retinas were a gift from Jun Yang (Moran Eye Center, Salt Lake City, UT).

Yeast Two-Hybrid Analysis

Yeast two-hybrid screening was performed using the GAL4-based two-hybrid system. Cloning vectors, yeast host cells, and reagents were

purchased from Clontech Laboratory (Palo Alto, CA). A retinal cDNA library was constructed from poly(A)⁺ RNA from C57BL/6 mouse retinas, and the cDNAs were inserted into the pACT2 plasmid vector downstream from the GAL4 activation domain. The bait plasmid was constructed by inserting a cDNA encoding the bait protein into the pGBKT7 plasmid vector downstream from the GAL4 DNA binding domain. The bait protein consisted of the C-terminus of mouse Rpgg^{ORF15} (amino acids 679–781). Reference to the numbering of exon ORF15 of the Rpgg^{ORF15} sequence in this report is based on GenBank accession number HQ260316. A sequential transformation protocol was used to introduce bait and library plasmids into yeast. Yeast AH109 cells were first transformed with the bait plasmid, and the bait protein expression was verified by immunoblot analysis. Competent cells were then prepared from a yeast clone harboring the bait plasmid and were transformed with the library plasmids. Positive colonies were isolated based on their ability to express nutritional markers HIS3 and ADE2 and the lacZ reporter, driven by different Gal4-responsive promoters, to minimize false positives from fortuitous activation of a particular promoter. Candidate plasmids were sequenced on an automated sequencer (ABI 3100; Applied Biosystems, Inc., Foster City, CA).

Reverse Transcription–Polymerase Chain Reaction

Total RNA was prepared from mouse retina using reagent (TRIzol; Invitrogen, Carlsbad, CA), and reverse transcription-polymerase chain reaction (RT-PCR) was performed using a RT-PCR kit (SuperScript III; Invitrogen) according to the manufacturer's instructions. PCR reactions were performed with DNA polymerase (PfuUltra II Fusion HS; Stratagene, La Jolla, CA). WiP1 (5'-ATGAACGCACAGCTGGACGGC-3') and WiP4R (5'-CTGATAGCCCTGAACCTTGCC-3') primers were used to amplify the full-length whirlin transcript. WiP1 and WiP14R (5'-CAGTAGTTGCATCAAACATTAGCTGCC-3') primers were used to amplify the whirlin NT1 transcript. WiP1 and Wi_intron7_P1R primers were used to amplify the whirlin NT2 transcript. The locations of all primers are illustrated in Figure 1C. PCR products were gel purified and cloned (StrataClone Ultra Blunt PCR Cloning Kit; Stratagene).

3' Rapid Amplification of cDNA Ends

Total RNA was prepared from mouse retina using reagent (TRI; Sigma-Aldrich, St. Louis, MO). RT-PCR was performed using a cDNA amplification kit (GeneRacer; Invitrogen) in accordance with the manufacturer's instructions. Whirlin transcripts were amplified by nested PCR using whirlin-specific 5' primers (WiP1 and WiP2; 5'-AGCTGCTCTTGCACCAGTACAGC-3') and two 3' primers (GeneRacer 3' Primer and GeneRacer 3' Nested Primer; Invitrogen). For cloning, 3' RACE products were gel purified and ligated with a PCR cloning kit (Zero Blunt TOPO; Invitrogen).

Cell Culture and Transfection

AAV293 cells were maintained in Dulbecco's modified Eagle's medium supplemented with 5% fetal bovine serum, penicillin (100 U/mL), and streptomycin (130 µg/mL) at 37°C in an atmosphere of 5% CO₂. Transient transfection was performed using the standard calcium phosphate method. Transfected cells were washed once with PBS and were homogenized in 50 mM Tris, pH 7.4, 150 mM NaCl, and 0.5% NP40. Cell lysates were cleared by centrifugation at 12,000g for 10 minutes, and the supernatants were used for subsequent immunoblot analysis or protein pull-down assays.

Protein Pull-Down Assays

N-terminal MBP fusion proteins containing the WhirlinNT1 variant (GenBank accession no., HQ148552), the whirlin PDZ₁ domain (amino acids 141–216; GenBank accession no., NP_082916.1), the whirlin PDZ₂ domain (amino acids 270–350), the region between the two PDZ domains (amino acids 217–269), or MBP alone were expressed in *Escherichia coli* Rosetta cells using the pMALC2X expression vector (New England Biolabs, Beverly, MA). To verify that equivalent

amounts of the specific MBP-fusion proteins and MBP protein alone were used, purified protein was analyzed by Bradford assay, and equimolar concentrations were calculated. A single Rpgg^{ORF15} transcript was obtained by RT-PCR using ORF15-specific primers and cloned using a PCR cloning kit (Zero Blunt TOPO; Invitrogen). After subcloning into a mammalian expression vector under the control of the CBA (CMV enhancer/chicken β-actin) promoter, the 75-kDa isoform was expressed by transient transfection in HEK293 cells. Increasing equimolar concentrations (0.625 mM, 1.875 mM, and 5.625 mM) of the MBP fusion proteins and MBP protein alone were immobilized on amylose resin and were incubated with HEK293 cell lysate expressing the 75-kDa Rpgg^{ORF15} variant for 2 hours at room temperature with gentle rocking. The beads were washed four times with binding buffer, resuspended as described, and assayed using anti-S1 antibody.

The C-terminal domain of mouse Rpgg^{ORF15} (amino acids 679–781 of exon 14/15), which was used as bait in the yeast two-hybrid screen, was cloned into the pMALC2X expression vector (Invitrogen). An N-terminal maltose-binding protein fusion containing the ORF15 C-terminal domain and MBP alone was expressed in *E. coli* Rosetta cells and purified. Purified protein was quantified using a Bradford assay, and equivalent molar concentrations were calculated. cDNAs for expression of the whirlinNT1 and long whirlin isoforms were obtained by RT-PCR, as described, and were subcloned into pcDNA3.1(+)/3xMyc mammalian expression vector. The full-length whirlin and whirlinNT1 variants were expressed in HEK293 cells, and extracts were equalized by immunoblot analysis with anti-myc tag antibody. Purified MBP fusion protein of increasing molar concentration (0.625 mM, 1.875 mM, and 5.625 mM) were immobilized on amylose resin and were incubated with equal amounts of full-length whirlin and whirlinNT1 for 2 hours at room temperature with gentle rocking. Purified MBP alone was used at the highest equimolar concentration (5.625 mM) as a negative control. The beads were washed four times with binding buffer (25 mM Tris, pH 7.4; 100 mM NaCl; 1 mM MgCl₂; 0.1% NP40). Bound proteins were resuspended in 30 µL of 2× SDS sample buffer with β-mercaptoethanol and were analyzed by immunoblot analysis using anti-myc tag antibody.

Coimmunoprecipitation

Retinal homogenate from 6-week-old Rpgg^{ORF15} knockout mice was incubated overnight at 4°C with either anti-S1 antibody or preincubated rabbit serum. The antibody-protein complex was immobilized on protein G (Dynabeads; Invitrogen) in accordance with the manufacturer's instructions. Coimmunoprecipitated protein was visualized by immunoblot using whirlin-specific primary antibody, which was conjugated to alkaline phosphatase for direct detection by chemiluminescence without subsequent incubation with a secondary antibody.

Antibodies

Mouse whirlin fragments (WiNT, amino acids 1–322; WiCT, amino acids 670–907; GenBank accession no., NP_082916.1) were inserted into the expression vector pMALC2X. Recombinant proteins were expressed as N-terminal MBP-fusion proteins in *E. coli* Rosetta cells. Recombinant proteins were purified on amylose resin and were used to immunize rabbits. Whirlin-specific antibodies were affinity-purified from antisera against their respective immunizing antigens immobilized in an agarose bead column (Aminolink; Pierce, Rockford, IL). Specificity of the antibodies was verified against *E. coli*-expressing fusion proteins and against whirlin cDNA clones transiently expressed in a mammalian expression system (HEK293). The polyclonal ORF15 antibody, generated by immunizing a guinea pig with a glutathione S-transferase (GST) fusion protein encompassing residues 140–228 of the mouse Rpgg^{ORF15} exon, and the rabbit polyclonal S1 antibody, specific for residues 494–563 of all Rpgg variants (GenBank accession no., NP_001171421.1), have previously been characterized.^{23,24}

Monoclonal rhodopsin antibody, rho-1D4, was a gift from Robert Molday (University of British Columbia, Vancouver, BC, Canada), and chicken anti-rootletin antibody was previously published.²⁵ Primary

TABLE 1. Whirlin Variants

Whirlin Variants	GenBank Accession No.	Exons	Product Size (amino acids)	Calculated Molecular Weight (kDa)
1	82916.1	*1b, 2, 3, 4a, 5, 6b, 7, 9, 10, 11a, 12, 13	907	96.0
2	1008791.1	*1b, 2, 3, 4a, 5, 6b, 7, 8b, 9, 10, 11a, 12, 13	918	98.0
3	1008792.1	*1b, 2, 3, 4b, 5, 6b, 7, 9, 10, 11a, 12, 13	911	97.0
4	1008793.1	*1b, 2, 3, 4a, 5, 6b, 7, 8b, 9, 10, 11b, 12, 13	906	96.5
5	1008794.1	1b, *6b, 7, 8b, 9, 10, 11a, 12, 13	476	50.7
6	1008795.1	1a, *6b, 7, 9, 10, 11a, 12, 13	465	49.3
7	1008796.1	1a, *7, 9, 10, 11a, 12, 13	404	42.2
8	1008797.4	*6a, 7, 9, 10, 11a, 12, 13	550	58.7
9	1008798.1	6a, 7, *8a, 9, 10, 11a, 12, 13	366	38.5
WhirlinN T1	HQ148552	*1b, 2, 3	322	34.3
WhirlinN T2	HQ148553	*1b, 2, 3, 4a, 5, 6b, 7	571	61.6

Description of known whirlin variants, including GenBank accession numbers, details of included exons, product sizes, and calculated molecular weights.

* Exon containing predicted start codon for each variant. The letters a and b after exon numbers denote slight variability in reported exons, which are not expected to affect the resultant peptide.

antibodies raised in rabbit were detected with a goat anti-rabbit IgG-horseradish peroxidase conjugate (Pierce), and mouse monoclonal antibodies were detected with a goat anti-mouse IgG-alkaline phosphatase conjugate (Pierce). Alexa fluorochrome-conjugated secondary antibodies for immunostaining were used (Molecular Probes, Inc., Eugene, OR).

Immunoblot Analyses

For immunoblot analyses, tissues were homogenized in buffer (50 mM Tris, pH 7.4, 150 mM NaCl, 0.5% NP40) containing a protease inhibitor cocktail (Sigma-Aldrich) and were centrifuged at 1000g for 2 minutes. Whirlin full-length and short, N-terminal transcripts were subcloned into a pCDNA3.1 vector for mammalian protein expression and were transfected into HEK293 cells as described. For denaturing gel electrophoresis, samples were mixed with 4× SDS sample buffer with β-mercaptoethanol, separated on 10% polyacrylamide gels, and transferred to polyvinylidene difluoride membranes (Immobilon-P; Millipore). After blocking the membrane in 5% skim milk in PBS with 0.1% Tween, immunoreactivities were detected by applying primary antibody overnight, followed by the appropriate secondary antibody for 2 hours. As a marker, a prestained standard (Precision Plus; Bio-Rad, Hercules, CA), ranging from 10 to 250 kDa to 25 kDa, was used.

Immunohistochemistry

For in situ detection of Rpgr and whirlin, eyes were embedded in optimal cutting temperature (OCT) compound without fixation and were snap frozen in liquid nitrogen. Cryosections at 10-μm thick were cut and collected on pretreated glass slides (Superfrost Plus; Fisher Scientific). Sections were stored at -20°C and were used within 2 to 3 days. Sections were briefly fixed in 4% paraformaldehyde before immunofluorescence staining, which was performed as previously described.^{5,24}

Dissociated Photoreceptors

Dissociated photoreceptor fragments were obtained by mechanical detachment from freshly dissected mouse retinas, as previously described.²⁶ In brief, retinas were suspended in Ringer solution and were gently homogenized by five passes through a disposable transfer pipette. Cell fragments were allowed to adhere for 5 minutes to pretreated glass slides (Superfrost Plus; Fisher Scientific). Adhered cell fragments were fixed for 5 minutes in ice-cold methanol, before proceeding with typical immunocytochemical staining as previously described.^{5,24}

RESULTS

Identification of Rpgr-Whirlin Interaction Using the Yeast-Two Hybrid System

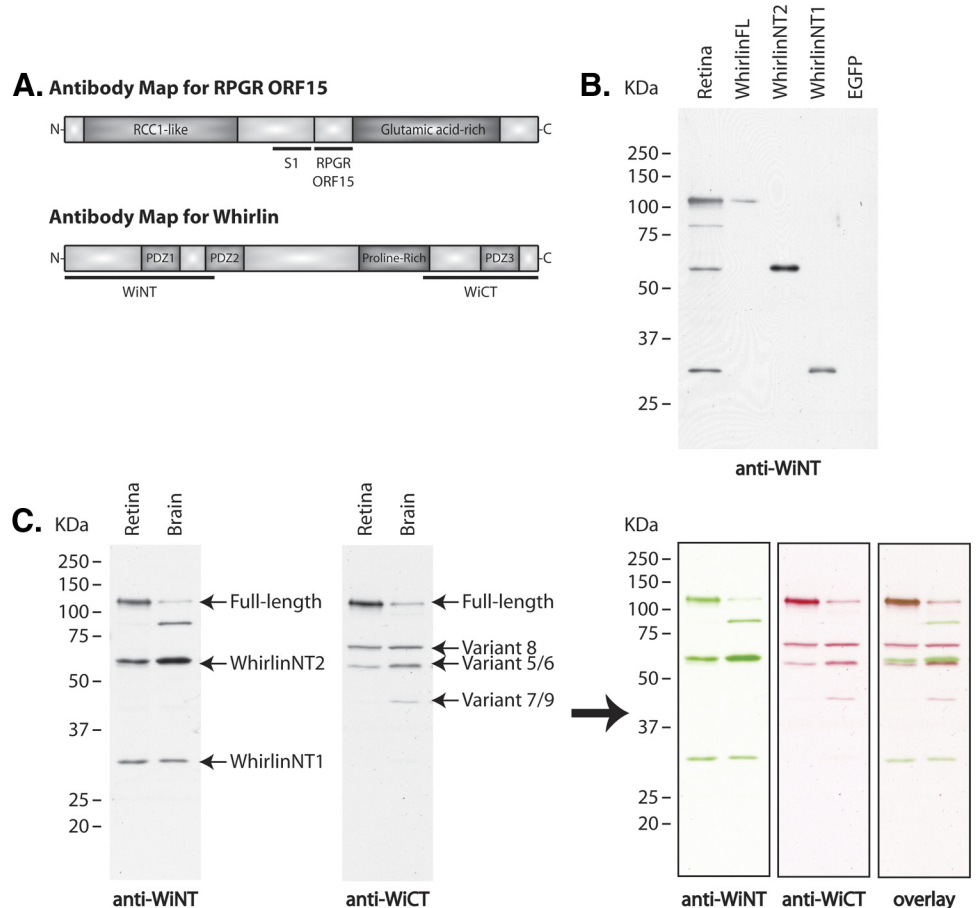
Since Rpgr^{ORF15} is preferentially expressed in photoreceptors and appears to be the functionally significant Rpgr variant,²⁷ we hypothesized that identifying proteins interacting with the C-terminal domain would provide clues to the physiological significance of these isoforms. We screened a C57BL/6 mouse retinal cDNA library by the yeast two-hybrid system using the C-terminus of mouse Rpgr^{ORF15} (mRpgr^{ORF15}) (amino acids 1241-1343) as bait (Fig. 1B). Of the 92 HIS³⁺, ADE2⁻, and lacZ⁺ colonies that were isolated and sequenced, 20 identical, independent clones represented the same gene sequence coding for the N-terminal region of whirlin, suggesting that RPGR^{ORF15} interacts physically with whirlin. We confirmed that the isolated library plasmid alone did not activate transcription of the reporter genes in yeast when transfected with a control bait protein.

Isolation of an N-terminal Whirlin Transcript by Sequencing Analysis of Retinal cDNA

Sequence analysis of the whirlin clone identified an N-terminal whirlin transcript. The highly conserved *whirlin* gene, which comprises 13 exons, is already known to have multiple long and short C-terminal isoforms (Table 1). Four distinct long isoforms, each of which has an estimated molecular weight of approximately 100 kDa, contain three PDZ domains (PDZ₁, PDZ₂, and PDZ₃) and a proline-rich region. The previously reported short C-terminal isoforms are the result of variable splicing and multiple start codons in exons 6, 7, and 8. They contain only the PDZ₃ domain and a proline-rich region^{20,28} (Fig. 1C).

The N-terminal transcript identified by our yeast two-hybrid screen, which was recently detected at the transcript but not at the protein level,²⁹ contains exons 1 through 3 followed by inclusion of the third intron and is the first known short N-terminal whirlin transcript. Translation of this variant is expected to result in abrupt truncation of the protein at the beginning of intron 3, resulting in a novel, N-terminal whirlin isoform, subsequently referred to as whirlinNT1 (GenBank accession no., HQ148552). To confirm the existence of this transcript in vivo, the cDNA was amplified from wild-type retinal tissue and was subsequently cloned and sequenced (Fig. 1C). In addition, we performed 3' RACE on wild-type retinal cDNA to confirm the existence of a mature mRNA transcript (Fig. 1D).

FIGURE 2. (A) Antibody maps for Rpgr and whirlin, and analysis of whirlin expression in the mouse retina. *Top:* illustration of the Rpgr^{ORF15} isoform structure and the location of domains used to generate polyclonal antibodies. S1 antibody detects all Rpgr isoforms; ORF15 detects only Rpgr^{ORF15}. *Bottom:* schematic representation of the whirlin long isoform structure and location of the domains used to generate polyclonal antibodies against the N-terminal and C-terminal ends. WiNT detects the long whirlin isoform and any potential short, N-terminal isoforms; WiCT also detects the long whirlin isoform and the previously reported short, C-terminal isoforms. (B, C) Characterization of whirlin antibodies and analysis of whirlin expression in the mouse retina and brain. (B) Immunoblot analysis of retinal homogenate and cell lysate from HEK293 cells transfected with the designated whirlin isoform. (C) Immunoblot analysis of retinal and cerebral homogenate from C57BL/6 wild-type mice. The WiNT antibody detects three major bands of approximately 110 kDa, 60 kDa, and 34 kDa in both the retina and the brain. We also detected an additional ~85-kDa band in the brain that is not consistently detected in the retina and has not been identified. The WiCT antibody detects three major bands of approximately 110 kDa, 70 kDa, and 60 kDa in both the retina and the brain, with an additional ~40-kDa band detected only in the brain. See Table 1 for GenBank accession numbers and a description of each known whirlin variant. Artificial colorization and merging of the images confirms that only the 110-kDa, long whirlin isoform is detectable by both antibodies and that all short N-terminal and C-terminal isoforms are detected only by their respective antibodies.



Identification of Other Novel, N-Terminal Whirlin Transcripts

After identifying a short, N-terminal whirlin isoform, we considered the possibility of other N-terminal variants. Using 3' RACE on wild-type retinal cDNA, we confirmed the existence of the whirlinNT1 transcript and identified a second N-terminal whirlin transcript, designated whirlinNT2 (Fig. 1D). The whirlinNT2 transcript includes exons 1 through 6 followed by part of intron 7, which results in truncation of the resultant peptide before the proline-rich domain (Fig. 1C). This transcript was subsequently confirmed by PCR amplification of retinal cDNA (Figs. 1C, 1D).

Confirmation of Whirlin Isoform Expression at the Protein Level in the Mouse Retina

To confirm the existence of the whirlinNT1 and whirlinNT2 transcripts at the protein level, we raised a polyclonal antibody, designated anti-WiNT, designed to recognize the long whirlin isoform and any potential N-terminal short whirlin isoforms (Fig. 2A). In retinal extracts, this antibody detected the 110-kDa, full-length whirlin isoform previously reported²⁹ (Fig. 2B). In addition, we detected two smaller variants of approximately 85 kDa and 60 kDa and a fourth variant of approximately 34 kDa (Fig. 2B). To confirm that these variants were isoforms of whirlin, the whirlinNT1 and whirlinNT2 transcripts were expressed in HEK293 cells (Fig. 2B). The anti-WiNT polyclonal antibody recognized the whirlinNT1 and

whirlinNT2 isoforms from these cell lysates (Fig. 2B), and the recombinant proteins matched the isoforms observed in retinal extracts. These results confirm the existence of the two novel whirlin transcripts at the protein level and provide an extensive characterization of the N-terminal whirlin splice variants expressed in the mouse retina. Despite extensive efforts, we were unable to identify a whirlin transcript corresponding to the 85-kDa band. Although we do not consistently detect this band in retinal extracts, it may be a degradation product, an N-terminal isoform we have not yet identified, a nonspecific antibody binding, or an oligomer. Given that whirlin has been reported to form homodimers,³⁰ the latter is a possible explanation.

To look for additional C-terminal isoforms, a polyclonal antibody was raised against the C-terminus of the long whirlin isoform, subsequently referred to as anti-WiCT. The domain used to generate this antibody is illustrated in the antibody map in Figure 2A. The calculated molecular weight of the long whirlin isoform is approximately 98 kDa; however, this isoform actually migrates at approximately 110 kDa. We therefore conclude that the additional isoforms recognized by the anti-WiCT antibody (Fig. 2C) correspond to the previously reported C-terminal short isoforms, with calculated molecular weights ranging between 38.5 kDa and 58.7 kDa (Table 1).

To further validate that the anti-WiNT and anti-WiCT antibodies both recognized the long whirlin isoform, the WiCT antibody was labeled with a horseradish peroxidase tag to eliminate the necessity for a secondary antibody during detection. This permitted sequential probing of the same blot with both antibod-

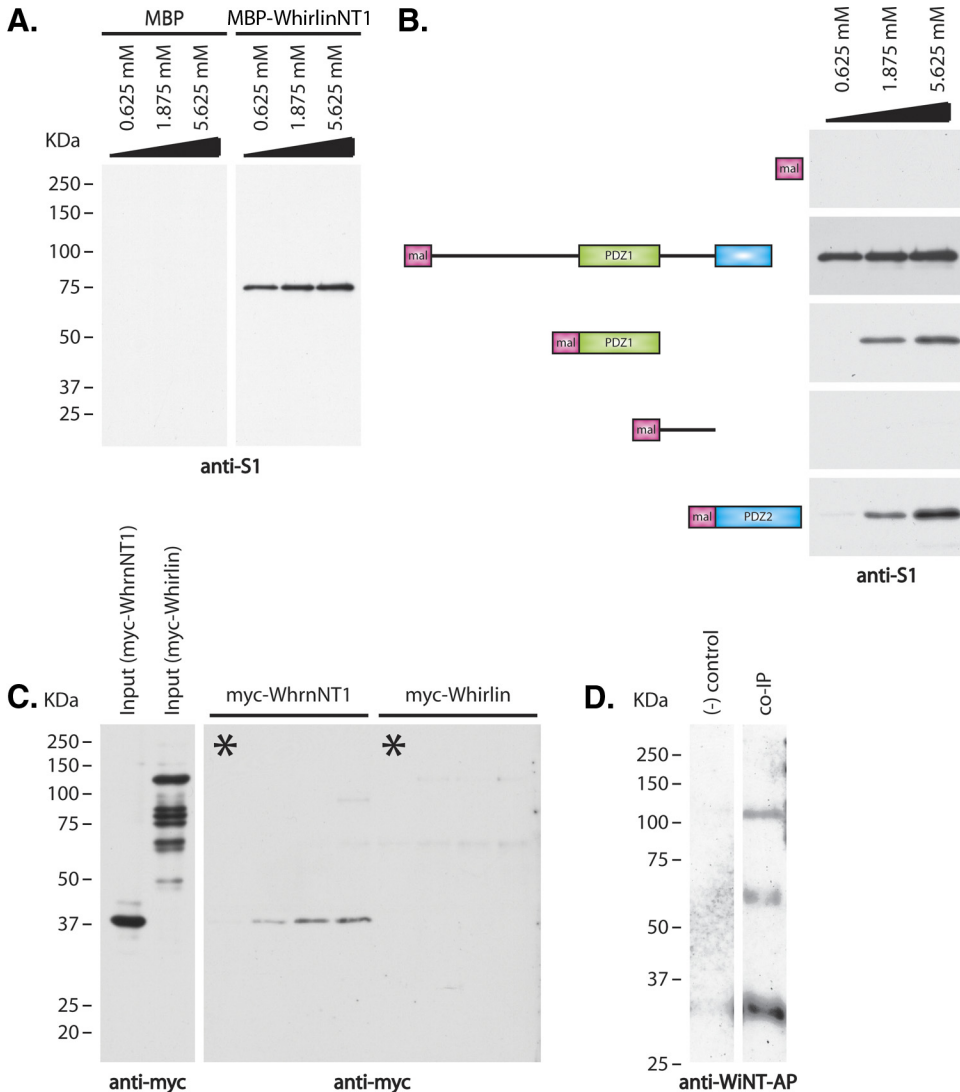


FIGURE 3. Confirmation and analysis of Rpggr^{ORF15}-whirlin interaction. (A) Extracts of transfected HEK293 cells expressing a 75-kDa Rpggr^{ORF15} isoform were incubated with immobilized MBP-tagged whirlinNT1 isoform (0.625 mM, 1.875 mM, and 5.625 mM) or MBP alone (0.625 mM, 1.875 mM, and 5.625 mM). Bound Rpggr was analyzed by immunoblot with the S1 antibody to identify Rpggr isoforms. (B) Schematic representation of the various whirlin constructs used and immunoblot analysis of pull-down assays used to identify Rpggr^{ORF15} binding domain. *From top:* MBP protein (negative control); MBP-whirlinNT1 isoform (positive control); MBP-whirlin PDZ₁ domain; MBP-whirlin inter PDZ₁/PDZ₂ domain; MBP-whirlin PDZ₂ domain. Increasing molar concentrations (0.625 mM, 1.875 mM, and 5.625 mM) of each fusion protein were immobilized on amylose resin and were incubated with equal amounts of HEK293 cells lysate expressing a 75-kDa Rpggr^{ORF15} isoform. (C) Comparison of Rpggr^{ORF15} interaction with the whirlinNT1 isoform and the long whirlin isoform. *Left:* myc-tagged whirlinNT1 and whirlin long isoforms from transfected HEK293 cells. The smaller bands in the whirlin long isoform lane are degraded protein detected by the myc antibody. *Right:* immunoblot of binding assay. Increasing amounts of MBP-ORF15 fusion protein were incubated with fixed amounts of either the myc-tagged whirlin NT1 or the myc-tagged long whirlin isoform. *Asterisk:* negative control in which MBP was substituted at the highest molar concentration of MBP-ORF15 fusion protein. (D) Immunoblot of coimmunoprecipitation to confirm Rpggr^{ORF15}-whirlin interaction in vivo. Rpggr was immunoprecipitated from *Rpgrip*

knockout retinal homogenate using anti-S1 antibody. Bound protein was analyzed by immunoblot using alkaline phosphatase-tagged anti-WiNT antibody. *Left:* negative control of immunoprecipitation using preincubated antisera in place of anti-S1 antibody. *Right:* immunoprecipitation using anti-S1 antibody.

ies, without detection of any background signal from the original antibody. We assigned colors and superimposed these images to emphasize that both anti-WiNT and anti-WiCT antibodies detect the long whirlin isoform and that each antibody detects a unique set of alternative, short whirlin isoforms (Fig. 2C).

Rpggr^{ORF15} Directly Interacts with the Novel USH2D Protein Isoform, WhirlinNT1

Having verified the presence of multiple whirlin polypeptides in the retina, the Rpggr^{ORF15}-whirlin interaction was first validated by MBP pull-down assay. We incubated a single 75-kDa mRPGR^{ORF15} isoform with a recombinant MBP-whirlinNT1 fusion protein or MBP alone. Increasing molar concentrations of MBP-whirlinNT1 incrementally increased the amount of bound Rpggr^{ORF15} (Fig. 3A). Interaction between m Rpggr^{ORF15} and the equivalent molar concentrations of MBP alone could not be detected.

Recombinant domains of whirlin were then used to identify the Rpggr^{ORF15} binding domain through another series of MBP pull-down assays. Four MBP-tagged constructs were tested: a construct containing a full PDZ₁ domain and a truncated PDZ₂ domain; the PDZ₁ domain only; the PDZ₂ domain only; and MBP fused to the linker region between the two PDZ domains (Fig. 3B). The whirlin PDZ₁ and PDZ₂ domains were identified

as independent binding sites for the C-terminus of Rpggr^{ORF15} (Fig. 3B). Importantly, Rpggr^{ORF15} exhibited the highest affinity for whirlin construct containing both PDZ domains, suggesting these two domains act cooperatively in whirlin binding. Interaction of neither the MBP-tagged linker domain nor MBP alone could be detected. Thus, we concluded that whirlin and Rpggr are interacting proteins and that whirlin binds by both PDZ₁ and PDZ₂ domains to the C-terminal end of Rpggr^{ORF15}.

Analysis of Rpggr^{ORF15} Interaction with the Full-Length Whirlin Isoform

To further characterize the significance of the Rpggr^{ORF15}-whirlin interaction, we sought to identify whether full-length whirlin was also capable of interacting with Rpggr^{ORF15}. We incubated the recombinant MBP-tagged Rpggr^{ORF15} C-terminal domain (amino acids 1241-1343) with equimolar concentrations of myc-tagged whirlinNT1 or myc-tagged full-length whirlin and immunoprecipitated with anti-myc antibodies (Fig. 3C). A recombinant MBP served as a control. As expected, neither whirlin isoform interacted with MBP alone (Fig. 3C, asterisks). Although we detected an interaction between myc-whirlinNT1 and MBP-tagged Rpggr^{ORF15} C-terminus, we were unable to detect an interaction between the full-length myc-

whirlin and MBP-tagged Rpgr^{ORF15} C-terminus (Fig. 3C). Two possibilities could explain the failure to detect binding between Rpgr^{ORF15} and full-length whirlin. First, the protein conformation of the full-length whirlin isoform may result in structural inhibition of its interaction with Rpgr^{ORF15}. Second, whirlin is characterized by the presence of three PDZ domains, which are protein scaffold domains known to form complexes with a number of other proteins. It is our hypothesis that the multitude of potential interactions between the three PDZ domains in full-length whirlin and other proteins in nonneuronal cell lysates may interfere with our binding assay. If this is correct, it may be possible to detect interactions between Rpgr^{ORF15} and full-length whirlin in retinal extracts.

In Vivo Confirmation of Rpgr^{ORF15}-Whirlin Interaction

To examine the interactions between Rpgr^{ORF15} and whirlin isoforms in vivo, Rpgr was immunoprecipitated from retinal homogenates using the anti-S1 antibody.^{23,24} Initial attempts to immunoprecipitate Rpgr from wild-type retinas failed to pull down detectable levels of either whirlin or Rpgr (data not shown). In wild-type retinas, Rpgr forms a high-affinity complex with Rpgrip at the connecting cilium, and very little soluble Rpgr protein is available for immunoprecipitation.²⁴ Rpgr was therefore immunoprecipitated from retinal lysates of *Rpgrip*^{-/-} knockout mice,^{22,24} and the bound whirlin was

detected with anti-WiNT antibodies (Fig. 3D). Coimmunoprecipitated protein was then analyzed by immunoblot analysis using anti-WiNT antibody (Fig. 2A). To eliminate direct interaction of the secondary antibody with the anti-S1/Rpgr complex, we tagged our anti-WiNT antibody with an alkaline phosphatase tag such that it could be directly detected by chemiluminescence substrate without subsequent incubation with a secondary antibody. Results from the coimmunoprecipitation assay confirmed our hypothesis that Rpgr^{ORF15} specifically interacts with the whirlinNT1 isoform in the mouse retina. In addition, we confirmed that Rpgr^{ORF15} exhibits a physiological interaction with full-length whirlin and the novel whirlinNT2 isoform (Fig. 3D). These results suggest that the failure to detect an in vitro interaction between Rpgr^{ORF15} and full-length whirlin is an artifact.

Rpgr^{ORF15} Colocalizes with Whirlin in the Mouse Retina

Rpgr is known to localize in the connecting cilia of both rod and cone photoreceptors.^{5,9,12,24} Although reports differ regarding the localization of whirlin,^{18,29,31,32} our initial hypothesis and subsequent interpretations are based on observations of whirlin within the connecting cilium, as measured by immunogold electron microscopy in both mouse and *Xenopus* photoreceptors,¹⁸ and that whirlin has been shown to precipi-

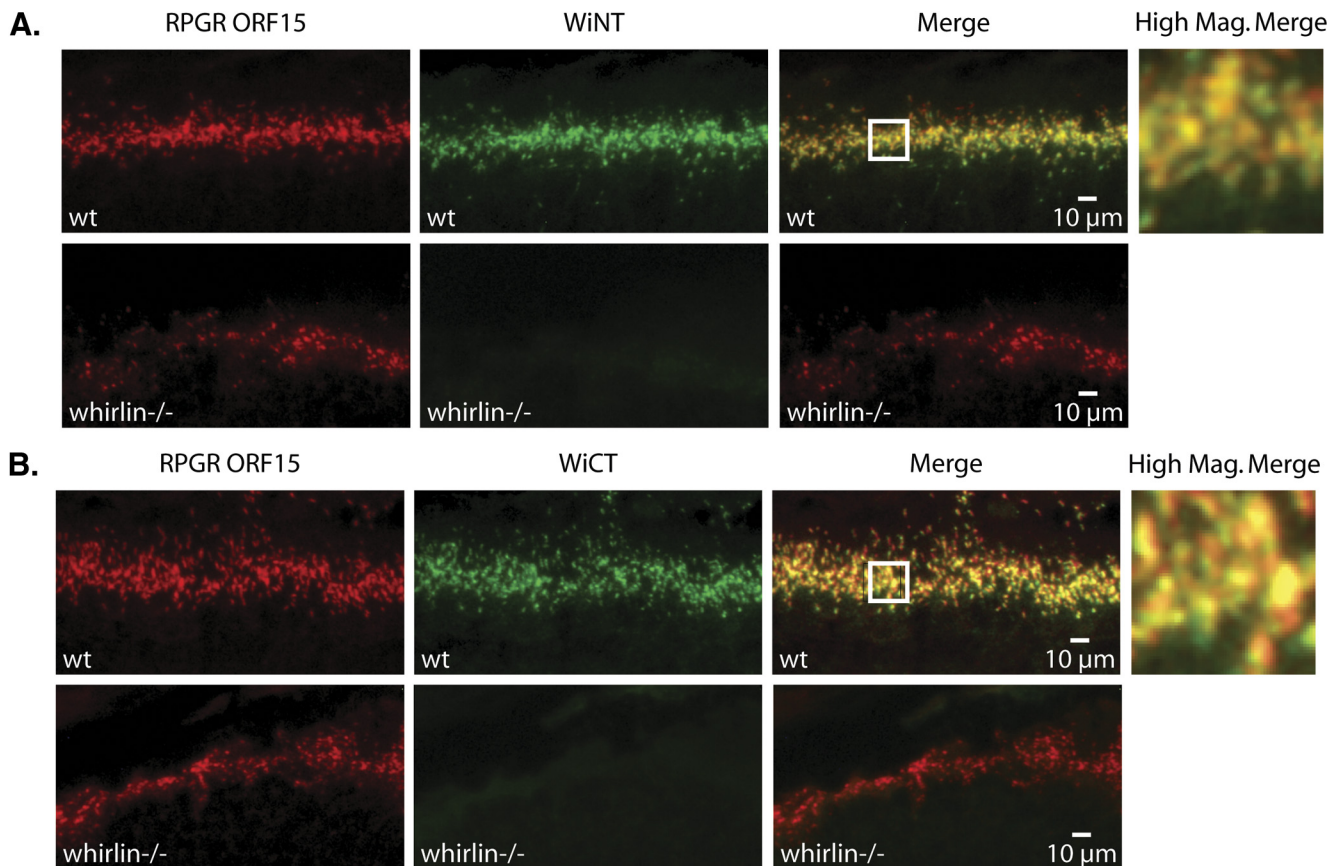


FIGURE 4. Colocalization of whirlin and Rpgr^{ORF15} in the mouse retina by immunohistochemical analysis. (A, top) Double staining of C57BL/6 wild-type retina with Rpgr ORF15 polyclonal antibody (red) and WiNT polyclonal antibody (green). Bottom: double staining of whirlin knockout retina with Rpgr ORF15 polyclonal antibody (red) and WiNT polyclonal antibody (green). (B, top) Double staining of C57BL/6 wild-type retina with Rpgr ORF15 polyclonal antibody (red) and WiCT polyclonal antibody (green). Bottom: double staining of whirlin knockout retina with Rpgr ORF15 polyclonal antibody (red) and WiCT polyclonal antibody (green). (A, B) The boxed region on the merged images indicates the region shown at right at higher magnification. The higher magnification merged images indicate that both whirlin antibodies partially colocalize with Rpgr^{ORF15} in the vicinity of the photoreceptor-connecting cilia.

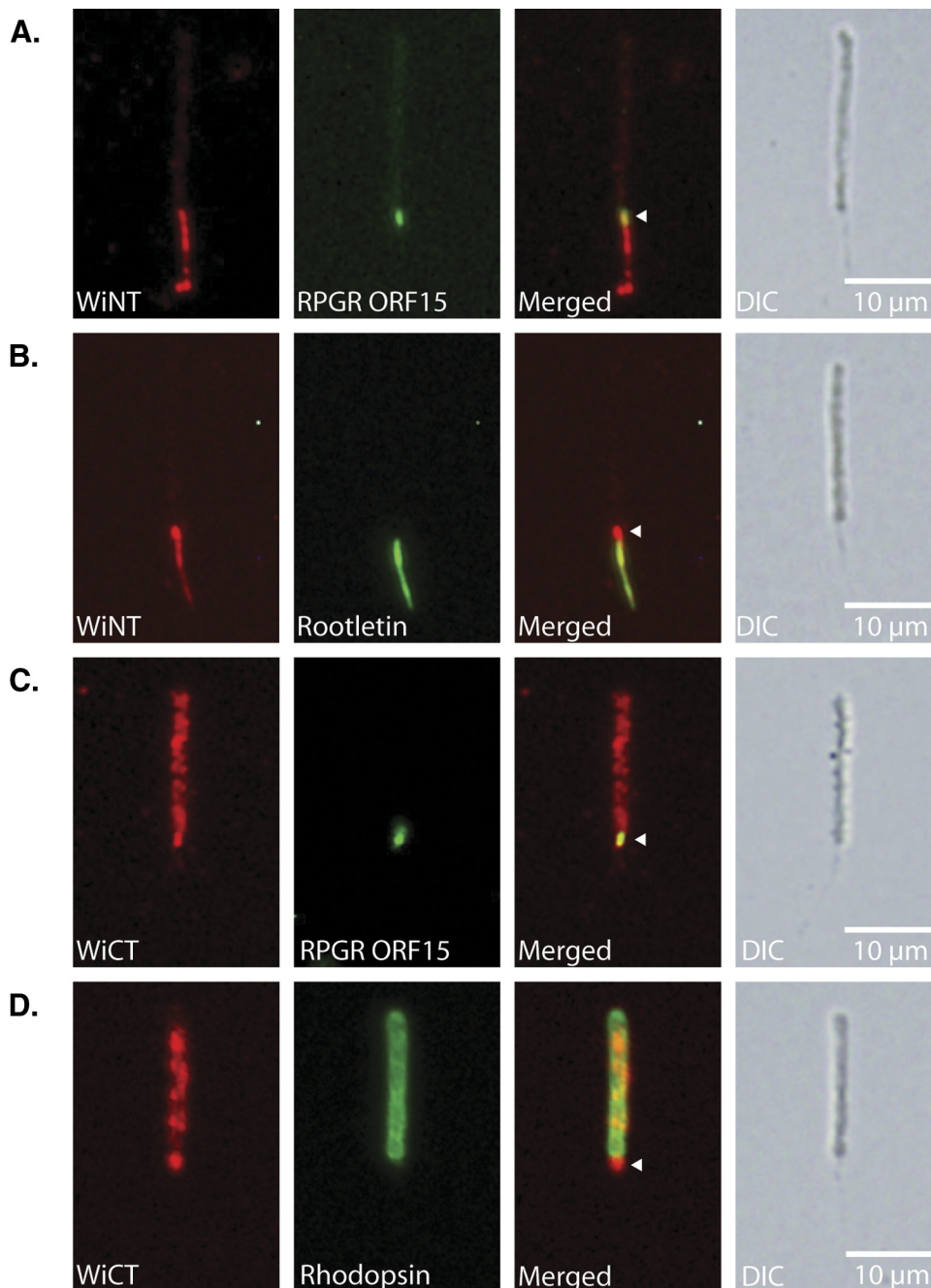


FIGURE 5. Subcellular localization of whirlin isoforms in dissociated retinal photoreceptors. (A) Double staining for whirlin N-terminal isoforms and Rpgr^{ORF15}. (B) Double staining for whirlin N-terminal isoforms and Rootletin. (C) Double staining for whirlin C-terminal isoforms and Rpgr^{ORF15}. (D) Double staining for whirlin C-terminal isoforms and rhodopsin. Arrowheads: areas of colocalization within the connecting cilium.

itate with other proteins found predominantly within the connecting cilium.^{18,31,32}

Immunohistochemical analysis of unfixed retinal cryosections detected whirlin in the vicinity of the connecting cilia by both the WiNT and WiCT antibodies. Significantly, whirlin colocalized with Rpgr^{ORF15} (Figs. 4A, 4B). At the light microscopy level, our results correspond well to numerous publications that show high-magnification images of whirlin colocalizing with markers of the connecting cilium. We were unable, however, to verify previous reports of whirlin in the outer plexiform layer or the outer limiting membrane.¹⁸

To confirm the specificities of the whirlin antibodies *in vivo*, we also performed immunohistochemistry staining on unfixed retinal cryosections from *whirlin* knockout mice (Figs. 4A, 4B). As expected, Whirlin immunoreactivity was not observed in *whirlin* knockout mice. In addition, localization of Rpgr^{ORF15} in the connecting cilia is not dependent on whirlin.

Our data indicate that whirlin extensively colocalizes with Rpgr^{ORF15} in the photoreceptor-connecting cilia and that ciliary localization of Rpgr^{ORF15} does not depend on whirlin.

Distribution of Whirlin in Dissociated Photoreceptors

To further examine the colocalization of Rpgr^{ORF15} and whirlin at a higher resolution, we performed double labeling for Rpgr^{ORF15} and whirlin on dissociated photoreceptors. Immunofluorescence studies on dissociated photoreceptors are commonly performed to provide better spatial resolution of certain proteins.^{5,23,33,34} This approach often provides better staining because of differences in the fixation methods and the availability of epitopes. Comparison of the immunofluorescence images double-labeled with our anti-WiNT and anti-Rpgr ORF15 antibodies confirmed colocalization of the interacting

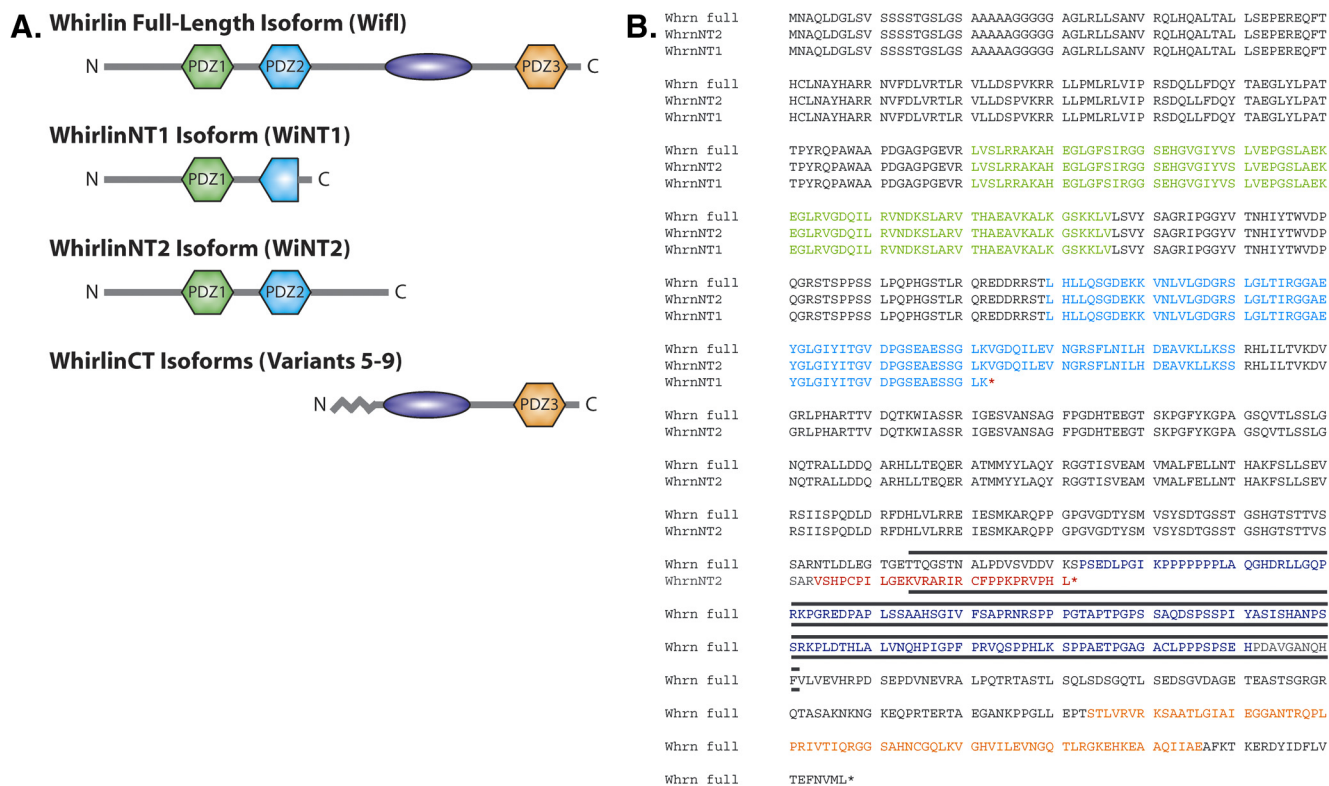


FIGURE 6. Comparison of the long whirlin isoform with the predicted short, N-terminal isoforms expressed in the mouse retina. **(A, B)** The three predicted PDZ domains (amino acid positions 141–216, 280–350, and 815–886) are shown in *green*, *cyan*, and *orange*, respectively, and the proline-rich domain (amino acid positions 573–712) is shown in *dark blue*. **(A)** Schematic representation of the mouse whirlin isoforms showing long, N-terminal, and C-terminal short isoforms. Each N-terminal short isoform (WhirlinNT1 and WhirlinNT2) is represented separately to illustrate domain variation, whereas the C-terminal short isoforms, which are all predicted to encode the same domains, are shown collectively. The *zigzag line* is shown to indicate variability in the N-terminus of the C-terminal short isoforms. **(B)** Amino acid sequence for the long whirlin isoform and novel N-terminal whirlin isoforms. Predicted stop codons for each isoform are indicated with an *asterisk*, and alternative amino acids are shown in *red*. The extent of the *whirler* deletion is marked by a *black line*.

proteins within the connecting cilium (Fig. 5A; arrowhead). In addition to localization in the connecting cilia, our WiNT antibody exhibited punctate staining along the rootlet, as is shown in the colocalization with anti-rootletin antibody in Figure 5B. We also coimmunolabeled dissociated photoreceptors using our anti-WiCT and anti-Rpgr^{ORF15} antibodies, which again confirmed colocalization of Rpgr^{ORF15} and whirlin in the photoreceptor-connecting cilia (Fig. 5C). Our anti-WiCT labeling was not restricted to the connecting cilium and exhibited a punctate staining pattern in the photoreceptor outer segment that colocalized with rhodopsin (Fig. 5D). We were unable to detect whirlin localization in the periciliary region with either antibody because of the physical disruption of the cell used to obtain dissociated photoreceptor fragments. Thus, immunostaining of dissociated photoreceptors not only confirms the colocalization of Rpgr^{ORF15} and whirlin in the connecting cilia, it demonstrates that the different whirlin isoforms show distinct localization patterns within photoreceptors and therefore may have distinct functions within the subcellular compartments of photoreceptors.

DISCUSSION

Mutations in *RPGR* are one of the most frequent causes of inherited retinal degeneration. Based on mutational analysis and previous studies of Rpgr null and transgenic mice, the photoreceptor-specific Rpgr^{ORF15} isoforms are essential to photoreceptor maintenance and survival. In this study, we identified the Usher protein whirlin as a novel interactor with

Rpgr and, by transcriptional and protein analysis of whirlin expression, identified two novel N-terminal short whirlin isoforms (Fig. 6). Our data also indicate that these short N-terminal variants and the previously reported short C-terminal variants have different subcellular localizations within photoreceptors and thus may retain discrete functions. The whirlin-Rpgr^{ORF15} interaction identified in this study provides the first evidence linking Rpgr^{ORF15} to the Usher protein network, thereby indirectly connecting Rpgr^{ORF15} to a number of other proteins also known to cause RP. The analogous retinal phenotypes associated with mutations in these loci indicate a physiologically significant interaction that may provide further evidence of the function of these proteins in photoreceptors.

WHRN/DFNB31 was first identified as a novel locus responsible for an autosomal recessive form of nonsyndromic congenital deafness, identified as DFNB31.²⁰ Recently, mutations in whirlin have been found to underlie Usher syndrome, type IID (USH2D), an autosomal recessive condition that manifests as both congenital hearing loss and visual impairment resulting from retinitis pigmentosa.^{35,36} Ebermann et al.²⁹ proposed that the genotype-phenotype correlation (nonsyndromic deafness vs. USH2D) may be dependent on the location of a given mutation within the whirlin gene locus. Although the first disease-causing mutations identified in humans truncated the protein close to its C-terminus and caused DFNB31, they reported compound heterozygosity affecting the integrity of the 5' end of the *WHRN* gene as the causative loci in a patient with USH2D. Their theory was further supported in a recent study²⁹ comparing a *whirlin* knockout mouse to the *whirler* mouse.

The *whirler* mouse has a large deletion in the 3' end of the *whirlin* gene (Fig. 6B) and is phenotypically similar to DFNB31 patients²⁸; however, targeted deletion of the *whirlin* gene, which affects both long and short C-terminal whirlin variants, results in both retinal and inner ear defects that resemble the human USH2D phenotype.²⁹ Our study, however, provides the first physiological evidence to suggest such phenotypic differences reflect the variable protein interactions, subcellular localization, and likely independent function of the short N-terminal and C-terminal whirlin isoforms.

First and foremost, our key finding is the identification of a novel interaction between whirlin and Rpgr^{ORF15}. Because Rpgr^{ORF15} interacts with the PDZ₁ and PDZ₂ domains of whirlin, our data imply that these N-terminal domains retain an important functional role in photoreceptors. Furthermore, identification of two short N-terminal whirlin isoforms suggests that not only do the N-terminal PDZ domains boast specific and distinct interactions, the differential expression of the whirlin gene produces both N-terminal and C-terminal variants. In contrast to the previously reported C-terminal variants, which encode the PDZ₃ domain and the proline-rich region, the first of these novel N-terminal isoforms encodes only the PDZ₁ domain and undergoes internal truncation within the PDZ₂ domain, whereas the second encodes both the PDZ₁ and the PDZ₂ domains (Fig. 6). This indicates that whirlin undergoes alternative splicing to produce variable isoforms, each with a unique combination of domains and potentially independent function.

In summary, the data in this study are consistent with previous reports that whirlin localizes in or around the photoreceptor-connecting cilia, where it has been shown to precipitate with other predominantly ciliary proteins,^{18,31,32} and they establish that whirlin physically interacts with the ciliary protein Rpgr^{ORF15}.^{5,9,12,24} Further investigation using immunoelectron microscopy may better resolve the localization of whirlin and elucidate whether Rpgr^{ORF15} and whirlin interact within the connecting cilia or whether Rpgr^{ORF15} interacts with whirlin in transit to the cilia. This study also shows the presence of two novel, N-terminal short whirlin variants at the mRNA and protein level and further validates the significance of the integrity of the 5' end of the *whirlin/DFNB31* gene in photoreceptor function and survival.

Future investigations into the relationship of Rpgr^{ORF15} and the Usher protein network may provide further insight into the function of the ORF15 isoforms and the physiology of this growing interactome, both of which are thought to function in controlling ciliary trafficking. Given the complexity of this protein network and the number of known interactions, further investigation of potential direct and indirect interactions between Rpgr and other members of the Usher protein complex may facilitate better understanding of the biological significance of these proteins.

Acknowledgments

The authors thank Michael Criscitiello for assistance with preparation of this manuscript and Jun Yang for the gift of the whirlin knockout mouse tissue samples.

References

- Meindl A, Dry K, Herrmann K, et al. A gene (*RPGR*) with homology to the RCC1 guanine nucleotide exchange factor is mutated in X-linked retinitis pigmentosa (RP3). *Nat Genet.* 1996;13:35–42.
- Vervoort R, Lennon A, Bird AC, et al. Mutational hot spot within a new RPGR exon in X-linked retinitis pigmentosa. *Nat Genet.* 2000;25:462–466.
- Kennan A, Aherne A, Humphries P. Light in retinitis pigmentosa. *Trends Genet.* 2005;21:103–110.
- Bunker CH, Berson EL, Bromley WC, Hayes RP, Roderick TH. Prevalence of retinitis pigmentosa in Maine. *Am J Ophthalmol.* 1984;97:357–365.
- Hong DH, Pawlyk BS, Shang J, Sandberg MA, Berson EL, Li T. A retinitis pigmentosa GTPase regulator (RPGR)-deficient mouse model for X-linked retinitis pigmentosa (RP3). *Proc Natl Acad Sci U S A.* 2000;97:3649–3654.
- Zhang Q, Acland GM, Wu WX, et al. Different RPGR exon ORF15 mutations in *Canids* provide insights into photoreceptor cell degeneration. *Hum Mol Genet.* 2002;11:993–1003.
- Berson EL, Gouras P, Gunkel RD, Myrianthopoulos NC. Rod and cone responses in sex-linked retinitis pigmentosa. *Arch Ophthalmol.* 1969;81:215–225.
- Sharon D, Sandberg MA, Rabe VW, Stillberger M, Dryja TP, Berson EL. RP2 and RPGR mutations and clinical correlations in patients with X-linked retinitis pigmentosa. *Am J Hum Genet.* 2003;73:1131–1146.
- Yan D, Swain PK, Breuer D, et al. Biochemical characterization and subcellular localization of the mouse retinitis pigmentosa GTPase regulator (mRpgr). *J Biol Chem.* 1998;273:19656–19663.
- Kirschner R, Rosenberg T, Schultz-Heienbrok R, et al. RPGR transcription studies in mouse and human tissues reveal a retina-specific isoform that is disrupted in a patient with X-linked retinitis pigmentosa. *Hum Mol Genet.* 1999;8:1571–1578.
- Hong DH, Li T. Complex expression pattern of RPGR reveals a role for purine-rich exonic splicing enhancers. *Invest Ophthalmol Vis Sci.* 2002;43:3373–3382.
- Khanna H, Hurd TW, Lillo C, et al. RPGR-ORF15, which is mutated in retinitis pigmentosa, associates with SMC1, SMC3, and microtubule transport proteins. *J Biol Chem.* 2005;280:33580–33587.
- Reiners J, van Wijk E, Marker T, et al. Scaffold protein harmonin (USH1C) provides molecular links between Usher syndrome type 1 and type 2. *Hum Mol Genet.* 2005;14:3933–3943.
- Reiners J, Nagel-Wolfrum K, Jurgens K, Marker T, Wolfrum U. Molecular basis of human Usher syndrome: deciphering the meshes of the Usher protein network provides insights into the pathomechanisms of the Usher disease. *Exp Eye Res.* 2006;83:97–119.
- Kremer H, van Wijk E, Marker T, Wolfrum U, Roepman R. Usher syndrome: molecular links of pathogenesis, proteins and pathways. *Hum Mol Genet.* 2006;15 Spec No 2:R262–R270.
- El-Amraoui A, Petit C. Usher I syndrome: unravelling the mechanisms that underlie the cohesion of the growing hair bundle in inner ear sensory cells. *J Cell Sci.* 2005;118:4593–4603.
- Adato A, Michel V, Kikkawa Y, et al. Interactions in the network of Usher syndrome type 1 proteins. *Hum Mol Genet.* 2005;14:347–356.
- Maerker T, van Wijk E, Overlack N, et al. A novel Usher protein network at the periciliary reloading point between molecular transport machineries in vertebrate photoreceptor cells. *Hum Mol Genet.* 2008;17:71–86.
- Tian G, Zhou Y, Hajkova D, et al. Clarin-1, encoded by the Usher Syndrome III causative gene, forms a membranous microdomain: possible role of clarin-1 in organizing the actin cytoskeleton. *J Biol Chem.* 2009;284:18980–18993.
- Mustapha M, Chouery E, Chardenoux S, et al. DFNB31, a recessive form of sensorineural hearing loss, maps to chromosome 9q32–34. *Eur J Hum Genet.* 2002;10:210–212.
- Ebermann I, Scholl HP, Charbel Issa P, et al. A novel gene for Usher syndrome type 2: mutations in the long isoform of whirlin are associated with retinitis pigmentosa and sensorineural hearing loss. *Hum Genet.* 2007;121:203–211.
- Zhao Y, Hong DH, Pawlyk B, et al. The retinitis pigmentosa GTPase regulator (RPGR)-interacting protein: subserving RPGR function and participating in disk morphogenesis. *Proc Natl Acad Sci U S A.* 2003;100:3965–3970.
- Hong DH, Pawlyk B, Sokolov M, et al. RPGR isoforms in photoreceptor connecting cilia and the transitional zone of motile cilia. *Invest Ophthalmol Vis Sci.* 2003;44:2413–2421.
- Hong DH, Yue G, Adamian M, Li T. Retinitis pigmentosa GTPase regulator (RPGR)-interacting protein is stably associated with the photoreceptor ciliary axoneme and anchors RPGR to the connecting cilium. *J Biol Chem.* 2001;276:12091–12099.

25. Yang J, Liu X, Yue G, Adamian M, Bulgakov O, Li T. Rootletin, a novel coiled-coil protein, is a structural component of the ciliary rootlet. *J Cell Biol.* 2002;159:431-440.
26. Muresan V, Joshi HC, Besharse JC. Gamma-tubulin in differentiated cell types: localization in the vicinity of basal bodies in retinal photoreceptors and ciliated epithelia. *J Cell Sci.* 1993;104(pt 4):1229-1237.
27. Hong DH, Pawlyk BS, Adamian M, Sandberg MA, Li T. A single, abbreviated RPGR-ORF15 variant reconstitutes RPGR function in vivo. *Invest Ophthalmol Vis Sci.* 2005;46:435-441.
28. Mburu P, Mustapha M, Varela A, et al. Defects in whirlin, a PDZ domain molecule involved in stereocilia elongation, cause deafness in the whirler mouse and families with DFNB31. *Nat Genet.* 2003;34:421-428.
29. Yang J, Liu X, Zhao Y, et al. Ablation of whirlin long isoform disrupts the USH2 protein complex and causes vision and hearing loss. *PLoS Genet.* 2010;6:e1000955.
30. Delprat B, Michel V, Goodyear R, et al. Myosin XVa and whirlin, two deafness gene products required for hair bundle growth, are located at the stereocilia tips and interact directly. *Hum Mol Genet.* 2005;14:401-410.
31. van Wijk E, van der Zwaag B, Peters T, et al. The DFNB31 gene product whirlin connects to the Usher protein network in the cochlea and retina by direct association with USH2A and VLGR1. *Hum Mol Genet.* 2006;15:751-765.
32. Kersten FF, van Wijk E, van Reeuwijk J, et al. Association of whirlin with Cav1.3 (alpha1D) channels in photoreceptors, defining a novel member of the usher protein network. *Invest Ophthalmol Vis Sci.* 2010;51:2338-2346.
33. Luby-Phelps K, Fogerty J, Baker SA, Pazour GJ, Besharse JC. Spatial distribution of intraflagellar transport proteins in vertebrate photoreceptors. *Vision Res.* 2008;48:413-423.
34. Sale WS, Besharse JC, Piperno G. Distribution of acetylated alpha-tubulin in retina and in vitro-assembled microtubules. *Cell Motil Cytoskeleton.* 1988;9:243-253.
35. Beaty TH, Boughman JA. Problems in detecting etiological heterogeneity in genetic disease illustrated with retinitis pigmentosa. *Am J Med Genet.* 1986;24:493-504.
36. Boughman JA, Vernon M, Shaver KA. Usher syndrome: definition and estimate of prevalence from two high-risk populations. *J Chronic Dis.* 1983;36:595-603.